2023 45th Annual International Conference of the IEEE Engineering in Medicine & Biology Society (EMBC) | 979-8-3503-2447-1/23/$31.00 ©2023 IEEE | DOI: 10.1109/EMBC40787.2023.10340077

Adapting Artifact Subspace Reconstruction Method for Single-Channel EEG using Signal Decomposition Techniques*

Netiwit Kaongoen and Sungho Jo, *Member, IEEE*

***Abstract*— Artifact removal from electroencephalography (EEG) data is a crucial step in the analysis of neural signals. One method that has been gaining popularity in recent years is Artifact Subspace Reconstruction (ASR), which is highly effective in eliminating large amplitude and transient artifacts in EEG data. However, traditional ASR is not possible to use with single-channel EEG data. In this study, we propose incorporating signal decomposition techniques such as ensemble empirical mode decomposition (EEMD), wavelet transform (WT), and singular spectrum analysis (SSA) into ASR, to decompose single-channel data into multiple components. This allows the ASR process to be applied effectively to the data. Our results show that the proposed single-channel version of ASR outperforms its counterpart Independent Component Analysis (ICA) methods when tested on two open datasets. Our findings indicate that ASR has significant potential as a powerful tool for removing artifacts from EEG data analysis.**

***Clinical Relevance*— This provided artifact removal technique for single-channel EEG.**

I. Introduction

Electroencephalogram (EEG) is a prevalent neuroimaging technique for observing neural activity. Due to its noninvasive nature and low cost, EEG is more user-friendly and adaptable to a wider range of applications compared to other neuroimaging methods [1]. Conventionally, EEG is performed by attaching small electrodes to the scalp using an electrical-conductive gel or paste, and fitting an elastic cap to secure the electrodes to the user's head. EEG has a wide range of potential applications beyond its traditional use in clinical and research settings. These include the use of EEG as daily-life brain monitoring tools that can detect certain abnormalities in brain activity, such as epileptic seizures [2], or provide neurofeedback to help individuals control and regulate their mental state [3]. Additionally, it can be used in brain-computer interface (BCI) technology, allowing individuals to control devices or communicate with others using their brain activity [4]. With advancements in technology, EEG systems have become increasingly accessible and wearable, making it possible to use them in real-world settings.

In practical applications, EEG is often susceptible to interferences and noises that can originate from both the user and the environment. These interferences can include other biological signals, such as electrooculogram (EOG), electromyogram (EMG), and electrocardiogram (ECG) from the user, as well as equipment noise and environmental factors such as vibrations and acoustic noise [5]. To address this issue, various noise cancellation and artifact removal techniques can be employed to enhance the quality of EEG recordings and make the data more reliable for analysis and interpretation. An example of such a technique is independent component analysis (ICA), a blind source separation method that separates the neural and artifact components from the EEG signal [6]. It is important to note that different techniques can be effective in removing noise from EEG recordings, but they also have their own limitations and assumptions. Therefore, it is up to the researcher to choose the algorithms that best suits the target application, taking into consideration the specific characteristics of the data and the research question.

Artifact Subspace Reconstruction (ASR) is a recent, component-based method for removing artifacts from data in a real-time, automated manner [7], [8]. It operates by calculating a principal component analysis (PCA) on covariance matrices, identifying and discarding components that exceed a predetermined threshold of variance from reference data, and reconstructing the data using the remaining components to produce a clean, artifact-free version. Previous studies showed that ASR can effectively clean multi-channel EEG data, especially from non-stationary large-amplitude, or transient artifacts that are commonly found in wearable EEG setups. In recent years, ASR has gained increasing attention and numerous studies have been conducted to evaluate its effectiveness in various research settings and propose ways to enhance the algorithm for improved robustness. For example, the work in [9] adapts the original ASR implementation by using Riemannian geometry for covariance matrix processing. The Riemannian ASR (rASR) is shown to outperform the original version in all three performance measures, including specificity, sensitivity, and efficiency. Research presented in [10] integrates Hebbian/anti-Hebbian neural networks into the ASR algorithm to create an adaptive ASR that eliminates the problem of the fixed threshold, which can lead to underperformance, especially when the quality of the reference data is poor. While the majority of ASR research has been conducted with high-density EEG recordings [11]-[13], it has also been validated that ASR is effective with EEG data acquired from wearable devices with a low number of EEG channels, as seen in studies [14] and [15].

A limitation of the current ASR technique is its inability to be applied to single-channel EEG systems. This is because the algorithm relies on calculating the EEG covariance matrix, which is not possible with single-channel data. This presents a

*This work was supported by Institute of Information & communications Technology Planning & Evaluation (IITP) grant funded by the Korea government (MSIT) (No. 2017-0-00432, Development of Non-invasive Integrated BCI SW Platform to Control Home Appliance and External Devices by User's Thought via AR/VR Interface).

N. Kaongoen and S. Jo are with Korea Advance Institute of Science and Technology, Daejeon, 34141, South Korea (email: ghiejo10jo@kaist.ac.kr; shjo@kaist.ac.kr. S. Jo is the corresponding author).

challenge for researchers and practitioners who work with single-channel EEG systems, such as those used in wearable devices [16]. In order to address this limitation and make the powerful artifact removal method of ASR more widely accessible and applicable, this study aims to explore the possibility of adapting the ASR algorithm for use with single-channel EEG. We propose a single-channel version of ASR that uses signal decomposition techniques to decompose single-channel EEG data into multiple signals, before applying the ASR process for artifact removal. The proposed method is evaluated using publicly available datasets, and the results will be compared to traditional single-channel ICA methods that utilize similar signal decomposition techniques. Signal decomposition techniques such as ensemble empirical mode decomposition (EEMD) [17], wavelet transform (WT) [18], and singular spectrum analysis (SSA) [19] will be considered, along with various hyper-parameter settings

II. Methodology

A. Artifact Subspace Reconstruction

In summary, ASR learns statistical properties from a given calibration data, which is a clean EEG data segment that is recommended to have a length of at least 30 seconds or 1 minute. Then, it compares those statistics to the statistics of the incoming data segment to identify and remove the artifact component, resulting in a cleaned EEG signal.

ASR consists of three main steps. In the first step, ASR segments the given calibration EEG data into multiple windows and calculates the root-mean-square (RMS) value of each window for each channel. It then identifies clean windows based on the RMS values that fall within a predetermined range. In the second step, ASR computes the covariance matrices from the clean data windows identified, and calculates the geometric median covariance matrix, U, to represent the clean covariance matrix sample. It then computes the mixing matrix, M, where $MM^T = U$, and performs PCA on M to obtain the eigenvectors matrix, V, and eigenvalues, D. At the end of this step, the clean data are projected into the component space. The mean, μ, and standard deviation, σ, of RMS values across all windows are computed for each component and used to define the rejection threshold $T_i = \mu_i + k\sigma_i$ for the i^{th} component, where k is a user-defined tuning hyperparameter. In the last step, the new, uncleaned EEG data, X_{New}, is undergone the same process as the previous step, and the components whose statistical properties exceed their rejection threshold T_i are replaced with zero vectors resulting in a clean eigenvector V_{clean}. Finally, ASR reconstructs and produces the clean EEG data X_{clean} using the equation:

$$X_{clean} = M(V^T_{clean}M)^+ V^T_{New} X_{New} \quad (1)$$

For in-depth information about the ASR algorithm, including technical details, please see [7] and [8].

B. Adapting ASR for Single-Channel EEG Data via Signal Decomposition Techniques

Similar to other blind-source-separation techniques such as ICA, traditional ASR techniques also require multi-channel EEG data. To overcome this limitation, we propose a single-channel version of the ASR method by incorporating signal decomposition techniques, specifically EEMD, WT, and SSA, to decompose the single-channel EEG data into multiple signals before applying the ASR process for artifact removal. For the WT method, we use the stationary wavelet transform (SWT) specifically to decompose the single-channel EEG data into multiple signals with the same sample length. Our proposed methods are named EEMD-ASR, WT-ASR, and SSA-ASR, respectively.

C. Validation

The proposed EEMD-ASR, WT-ASR, and SSA-ASR methods are validated using two open datasets. The first dataset, the Physiobank motion artifact dataset [20], [21], consists of 24 recordings where EEG signal was acquired from two electrodes that are closely placed together, resulting in highly correlated data. High-amplitude, transient motion artifacts were induced randomly in one of the electrodes by pulling its cable at approximately 2-minute intervals. The total length of the recordings was 9 minutes, and the sampling rate was originally 2048 Hz but was downsampled to 256 Hz to lower the computation cost. The data were preprocessed with a notch and 1-50 Hz bandpass filters to remove common noise. The first 1-minute EEG data segment of each recording was used as the calibration data for the ASR process. The disturbed channel was used as the target artifact-contaminated single-channel EEG data and the undisturbed channel as the ground truth for evaluation.

The second dataset is a semi-simulated EEG/EOG dataset [22], which combines EOG data linearly with EEG data to create semi-simulated EOG-contaminated EEG data. It comprises 55 EEG recordings, each containing 19 channels. The data were acquired at a sampling rate of 200 Hz. EEG recordings with a data length shorter than 30 seconds were discarded, resulting in a total of 33 EEG recordings. In this study, each channel of each recording was treated as an individual single-channel EEG sample. All data underwent the same filtering steps as the first dataset. Due to its short recording time, Gaussian noise with a standard deviation of 1 was added to the pure EEG data and used as the calibration data for the ASR method. Unprocessed pure EEG data were used as the ground truth for evaluation.

Three measurements were used to evaluate the effectiveness of the artifact removal process:

1) Improvement in Correlation Value (ΔR): The correlation between the ground truth EEG epoch (EEG_{Ref}) and the EEG epoch before (EEG_{Art}) and after the ASR process (EEG_{ASR}) are calculated. Then ΔR is defined as:

$$\Delta R = \mathrm{Corr}(EEG_{Ref}, EEG_{ASR}) - \mathrm{Corr}(EEG_{Ref}, EEG_{Art}) \quad (2)$$

where Corr(.) is the operation to calculate the correlation between two signals.

2) Improvement in Signal-to-Noise ratio (ΔSNR): In this work, the Signal-to-Noise ratio (SNR) of an EEG epoch is defined as:

$$SNR_{EEG} = 10 \log_{10}(\mathrm{Var}(EEG)/\mathrm{Var}(EEG\text{-}EEG_{Ref}) \quad (3)$$

where Var(.) calculates the variance of the input signal. SNR values are calculated for both EEG_{Art} and EEG_{ASR}, and ΔSNR is defined as:

$$\Delta SNR = SNR_{ASR} - SNR_{Art} \quad (4)$$

3) Improvement in Mean Square Error (ΔMSE): Similar to the other two measurements, ΔMSE calculates the improvement in the mean-square error (MSE) to the reference signal before and after the ASR process. It is defined as:

$$\Delta\text{MSE} = \text{MSE}(EEG_{Ref}, EEG_{ASR}) - \text{MSE}(EEG_{Ref}, EEG_{Art}) \quad (5)$$

where MSE(.) computes the MSE values between two signals.

D. Experimental setup

We applied the proposed single-channel ASR methods to both datasets with two hyperparameters: the number of decomposition levels, which ranges from 2 to 6 for EEMD-based and WT-based methods, and 2 to 16 for SSA-based method, and the threshold tuning parameter k for the ASR process, which ranges from 1 to 30. The default window length for the ASR method (500 ms) was used, and the EEG samples were processed in non-overlapping segments of 3 seconds at a time. We then averaged the values of three evaluation measurements across all samples and compared the results of the proposed methods to those of well-known single-channel ICA artifact removal algorithms, namely EEMD-ICA [6], WT-ICA [6], and SSA-ICA [24]. For the ICA-based methods, we iteratively removed all components that improved the correlation between the reference and processed signal to reconstruct the artifact-free signals.

III. Results and Discussion

The performance of each artifact removal method is shown in Table 1. The results shown in the table are the best results among all runs with different hyperparameters. It is important to note that the best results for the three evaluation measurements may not have been obtained from the same set of hyperparameters.

The validation results using the Physiobank Motion Artifact dataset showed that our proposed methods outperformed their ICA-based counterparts in all three evaluation measurements. The WT-ASR method showed the highest performance in all three measurements with values of 0.2770, 14.8686, and 10.4130 for ΔR, ΔSNR, and ΔMSE, respectively. Among the ICA-based methods, the ΔR of the WT-ICA method was higher than the EEMD-ASR and SSA-ASR methods, and its ΔMSE was also higher than the EEMD-ASR method. This suggests that the WT might be a better choice of signal decomposition method for handling high-amplitude, transient motion artifacts that are present in data from the Physiobank dataset. The SSA-ASR method outperformed the EEMD-ASR method in all three measurements, but this was not the case for SSA-ICA and EEMD-ICA methods, making the comparison between the EEMD and SSA signal decomposition methods inconclusive for this type of artifact.

The results from the semi-simulated EOG/EEG dataset revealed a distinct trend compared to the results from the Physiobank dataset. Although the ASR-based methods yielded the best results in all three measurements, not all proposed methods performed better than their ICA-based counterparts. The highest values of ΔR, ΔSNR, and ΔMSE were 0.1960 (SSA-ASR), 15.878 (EEMD-ASR), and 6.8592 (EEMD-ASR), respectively. The lower results compared to the Physiobank dataset were likely due to the larger amplitude of motion artifacts compared to the artifacts from the EOG signal.

TABLE I. Validation Results For The Proposed Single-Channel ASR Artifact Removal Methods And Single-Channel ICA-Based Methods. The Best Performance For Each Measurement Is Highlight In **Bold** Style.

Dataset	*Method*	*ΔR*	*ΔSNR*	*ΔMSE*
Physiobank Motion Artifact Dataset	EEMD-ASR	0.2305	14.6598	9.5141
	WT-ASR	**0.2770**	**14.8686**	**10.4130**
	SSA-ASR	0.2654	14.7843	10.1143
	EEMD-ICA	0.2271	13.1584	8.2743
	WT-ICA	0.2705	14.3765	9.7538
	SSA-ICA	0.2292	11.6732	6.2965
Semi-Simulated EEG/EOG Dataset	EEMD-ASR	0.1766	**15.8785**	**6.8592**
	WT-ASR	0.1427	15.0460	5.8926
	SSA-ASR	**0.1960**	15.0978	6.2899
	EEMD-ICA	0.1481	14.5129	5.7863
	WT-ICA	0.1779	14.3551	5.9093
	SSA-ICA	0.1952	14.0806	6.1685

Another clear observation is that the WT-ASR method, which performed best on the Physiobank dataset, performed the worst among the three proposed methods. This could be attributed to the limitation in the length of the EEG data segment, which resulted in a limited decomposition level of the WT method at 3. When the length of the data segment was increased from 3 to 6 seconds, the maximum decomposition level increased to 4, and the best ΔR was greatly increased from 0.1427 to 0.2070. Despite this improvement, there was no increase in ΔSNR or ΔMSE values. Although the length of the EEG data segment does not directly impact the performance of the ASR algorithm, certain signal decomposition techniques necessitate a minimum data length to accurately decompose the signal into a desired number of components. In BCI, short EEG segments are used to achieve fast command delivery. In contrast, other applications such as mental state monitoring may benefit from longer EEG segments for improved signal decomposition. It is important to consider the length of the EEG segment in conjunction with other hyperparameters when applying this single-channel ASR to a specific application.

To examine the effect of the ASR threshold, k, and the decomposition level on the performance, we plot the ΔR results from the best methods in Physiobank (WT-ASR) and EEG/EOG dataset (SSA-ASR). Fig. 1(a) shows the ΔR results with different values of k and a fixed decomposition level, while Figure 1(b) displays the ΔR results with different values of the decomposition level and a fixed k value. The fixed values for k and decomposition level correspond to the values that yielded the best ΔR results as shown in Table 1. According to the results, the ΔR metric steadily increased and peaked at k=5 for the Physiobank dataset and k=4 for the EEG/EOG dataset, before gradually decreasing as the ASR threshold increased. The peak of the ΔR results at a smaller value of k in the EEG/EOG dataset may be attributed to the fact that the artifacts from EOG, such as eye movements, tend to have smaller amplitudes compared to the motion artifacts present in the Physiobank dataset. Regarding the decomposition level, Fig. 1 (b) shows that the results improved as we increased the decomposition level for both methods in both datasets. This trend was also generally observed for the other signal

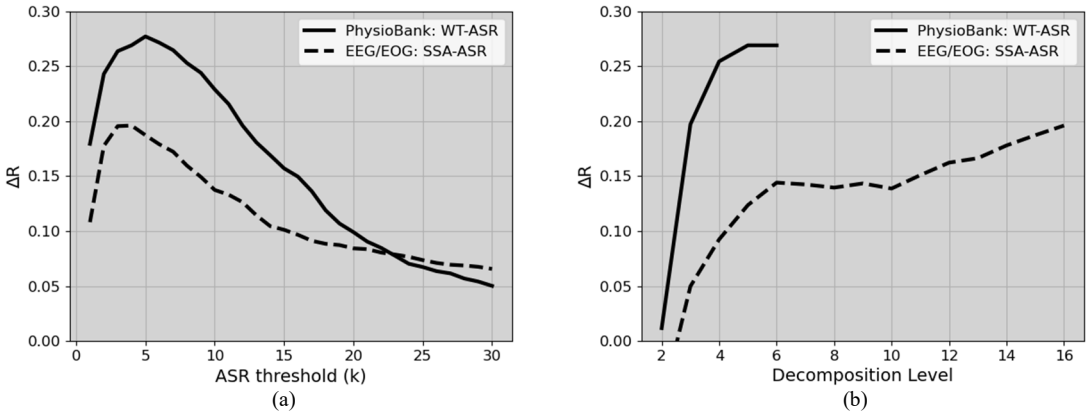

Figure 1. The improvement in correlation value (ΔR) of the WT-ASR method on the Physiobank Motion Artifact dataset for different values of the ASR threshold (k) and decomposition level, as shown in subplots (a) and (b) respectively.

decomposition techniques used in this study. This result indicates that a higher signal decomposition level is likely to improve performance, but one must also consider the length of the data segments to achieve an appropriate level of decomposition, as previously discussed. It is also important to weigh the trade-off between performance and computing cost when selecting the value of this hyperparameter, to ensure that it is suitable for the target application.

In conclusion, our method successfully adapted the ASR algorithm to make it usable with single-channel EEG data. The results showed that our method achieved performance that was equal to or better than well-known single-channel ICA-based methods. The use of signal decomposition techniques was key in achieving this success. In future work, we plan to test the algorithm with a variety of different types of artifacts and explore the potential for incorporating other methods to further improve performance. Overall, ASR has proven to be very effective and has great potential for artifact removal in EEG data. We believe that this method may become a valuable tool for researchers and practitioners working with EEG data.

REFERENCES

[1] S. Sanei and J. A. Chambers, "EEG signal processing," *John Wiley & Sons*, 2013.

[2] J. Gotman, "Automatic recognition of epileptic seizures in the EEG." Electroencephalography and clinical Neurophysiology 54.5 (1982): 530-540.

[3] BH Kim, S. Jo, and S. Choi, "ALIS: Learning affective causality behind daily activities from a wearable life-log system," IEEE Transactions on Cybernetics (2021).

[4] N. Kaongoen, J. Choi, and S. Jo, "A novel online BCI system using speech imagery and ear-EEG for home appliances control," Computer Methods and Programs in Biomedicine 224 (2022): 107022.

[5] Urigüen, Jose Antonio, and Begoña Garcia-Zapirain. "EEG artifact removal—state-of-the-art and guidelines." Journal of neural engineering 12.3 (2015): 031001.

[6] Mijović, Bogdan, et al. "Source separation from single-channel recordings by combining empirical-mode decomposition and independent component analysis." IEEE transactions on biomedical engineering 57.9 (2010): 2188-2196.

[7] Kothe, Christian Andreas Edgar, and Tzyy-Ping Jung. "Artifact removal techniques with signal reconstruction." U.S. Patent Application No. 14/895,440.

[8] T. R. Mullen, et al, "Real-time neuroimaging and cognitive monitoring using wearable dry EEG." IEEE Transactions on Biomedical Engineering 62.11 (2015): 2553-2567.

[9] S. Blum, "A Riemannian modification of artifact subspace reconstruction for EEG artifact handling." Frontiers in human neuroscience 13 (2019): 141.

[10] BY. Tsai, et al, "Development of an adaptive artifact subspace reconstruction based on hebbian/anti-hebbian learning networks for enhancing bci performance." IEEE Transactions on Neural Networks and Learning Systems (2022).

[11] CY. Chang, et al, "Evaluation of artifact subspace reconstruction for automatic EEG artifact removal." 2018 40th Annual International Conference of the IEEE Engineering in Medicine and Biology Society (EMBC). IEEE, 2018.

[12] M. Plechawska-Wojcik, M. Kaczorowska, and D. Zapala, "The artifact subspace reconstruction (ASR) for EEG signal correction. A comparative study." International Conference on Information Systems Architecture and Technology. Springer, Cham, 2018.

[13] CY Chang, et al, "Evaluation of artifact subspace reconstruction for automatic artifact components removal in multi-channel EEG recordings." IEEE Transactions on Biomedical Engineering 67.4 (2019): 1114-1121.

[14] V. P. Kumaravel, et al, "Efficient artifact removal from low-density wearable EEG using artifacts subspace reconstruction." 2021 43rd Annual International Conference of the IEEE Engineering in Medicine & Biology Society (EMBC). IEEE, 2021.

[15] A. Cataldo, "A Method for Optimizing the Artifact Subspace Reconstruction Performance in Low-Density EEG." IEEE Sensors Journal 22.21 (2022): 21257-21265.

[16] K. Crowley, et al, "Evaluating a brain-computer interface to categorise human emotional response." 2010 10th IEEE International Conference on Advanced Learning Technologies. IEEE, 2010.

[17] Z. Wu, and N. E. Huang, "Ensemble empirical mode decomposition: a noise-assisted data analysis method." Advances in adaptive data analysis 1.01 (2009): 1-41.

[18] G. P. Nason, and B. W. Silverman, "The stationary wavelet transform and some statistical applications." Wavelets and statistics. Springer, New York, NY, 1995. 281-299.

[19] H. Hassani, "Singular spectrum analysis: methodology and comparison." (2007): 239-257.

[20] K. T. Sweeney, et al, "A methodology for validating artifact removal techniques for physiological signals." IEEE transactions on information technology in biomedicine 16.5 (2012): 918-926.

[21] K. T. Sweeney, S. F. McLoone, and T. E. Ward, "The use of ensemble empirical mode decomposition with canonical correlation analysis as a novel artifact removal technique." IEEE transactions on biomedical engineering 60.1 (2012): 97-105.

[22] M. A. Klados, and P. D. Bamidis. "A semi-simulated EEG/EOG dataset for the comparison of EOG artifact rejection techniques." Data in brief 8 (2016): 1004-1006.

[23] A. K. Maddirala and R. A. Shaik. "Separation of sources from single-channel EEG signals using independent component analysis." IEEE Transactions on Instrumentation and measurement 67.2 (2017): 382-393.